Draft version March 1, 2012
Preprint typeset using LaTeX style emulateapj v. 5/2/11

arXiv:1202.6367v1 [astro-ph.GA] 28 Feb 2012

UPDATE ON THE NATURE OF VIRGO OVERDENSITY

Ana Bonaca[1, 2], Mario Jurić[3, 4], Željko Ivezić[5], Dmitry Bizyaev[6], Howard Brewington[6], Elena Malanushenko[6], Viktor Malanushenko[6], Daniel Oravetz[6], Kaike Pan[6], Alaina Shelden[6], Audrey Simmons[6], Stephanie Snedden[6]

Draft version March 1, 2012

ABSTRACT

We use the Eighth Data Release of Sloan Digital Sky Survey (SDSS DR8) catalog with its additional sky coverage of the southern Galactic hemisphere, to measure the extent and study the nature of the Virgo Overdensity (VOD; Jurić et al. 2008). The data show that the VOD extends over no less than 2000 deg^2, with its true extent likely closer to 3000 deg^2. We test whether the VOD can be attributed to a tilt in the stellar halo ellipsoid with respect to the plane of the Galactic disk and find that the observed symmetry of the north-south Galactic hemisphere star counts excludes this possibility. We argue that the Virgo Overdensity, in spite of its wide area and cloud-like appearance, is still best explained by a minor merger. Its appearance and position is qualitatively similar to a near peri-galacticon merger event and, assuming that the VOD and the Virgo Stellar Stream share the same progenitor, consistent with the VSS orbit determined by Casetti-Dinescu et al. (2009).

Subject headings: Galaxy: structure — Galaxy: halo — Galaxy: formation

1. INTRODUCTION

A growing number of observational campaigns over the last decade showed the richness of substructure in the Milky Way halo. The most vivid discoveries of ongoing accretion onto the Galaxy include the Sagittarius dwarf and its tidal streams (Ivezić et al. 2000; Yanny et al. 2000; Vivas et al. 2001; Majewski et al. 2003, among others), the Monoceros stellar stream (Newberg et al. 2002; Rocha-Pinto et al. 2003), as well as numerous smaller streams and dwarf galaxies abundant in the so-called "field of streams" (Belokurov et al. 2006). Evidence of ongoing mergers has also been detected in the halo of M31 (Ibata et al. 2001; Ferguson et al. 2002; Morrison et al. 2003; Zucker et al. 2004; Kalirai et al. 2006; Fardal et al. 2007), providing further support for the importance of hierarchical merging in galaxy formation.

Even if one is ultimately interested in the processes of galaxy formation in general, the study and understanding of these processes in the Milky Way remains advantageous in many aspects. For example, the proximity of stars and substructures in the Galaxy allows data collection at high resolution, which can be directly tested against predictions from simulations.

In this work, we concentrate on the Virgo Overdensity (VOD; Jurić et al. 2008), a cloud-like overdensity of stars spanning distances between $10-20$ kpc. Parts of the VOD were initially identified as an overdensity of RR Lyrae stars confined to a small region in the Quasar Equatorial Survey Team survey (Vivas et al. 2001), followed by an identification as an overdensity of main sequence turnoff stars in the same direction (Newberg et al. 2002). However, it was not until the advent of wide-area surveys such as the Sloan Digital Sky Survey (SDSS; York et al. 2000) that the size of the VOD feature was fully recognized (Jurić et al. 2008). In particular, using a large photometric sample of main sequence stars, Jurić et al. (2008) have shown that the VOD extends over at least 1000 deg^2, spans heliocentric distances between $6 < D < 20$ kpc, and also shows as an overdensity of M giants in the Two Micron All Sky Survey (2MASS; Skrutskie et al. 2006). Based on their $u-g$ band color, they further argued for low metallicity of its constituent stars. This is consistent with the spectroscopic determination by Duffau et al. (2006) ([Fe/H]$=-1.9$), who identified a velocity peak of RR Lyrae stars in the same direction, naming it the "Virgo Stellar Stream" (VSS)[7]. Subsequent kinematic studies showed that there may be individual filaments within the VOD/VSS region (Vivas et al. 2008), likely to belong to more than one stream. The current knowledge of VOD/VSS properties is summarized in Table 1.

Despite these extensive studies, there is still no definitive answer on the origin of the VOD/VSS nor of its extent. Since the stars are metal poor, but cover a wide range of metallicities, both Duffau et al. (2006) and Jurić et al. (2008) have argued it to be the debris of a tidally disrupted dwarf spheroidal galaxy. Supporting this hypothesis, Casetti-Dinescu et al. (2009) showed that orbit of an RR Lyrae star associated with the VSS, derived from proper motion and radial velocity observations, is consistent with a merging scenario in its early phase. An alternative, which would explain the unusually large angular size of the VOD, is that the overdensity may not be due to a merger but a misinterpretation of a

---

[1] Department of Astronomy, Yale University, New Haven, CT 06511; ana.bonaca@yale.edu
[2] Department of Physics, Faculty of Science, University of Zagreb, Croatia
[3] Institute for Theory and Computation, Harvard-Smithsonian Center for Astrophysics, Cambridge, MA 02138; mjuric@cfa.harvard.edu
[4] Hubble Fellow
[5] Department of Astronomy, University of Washington, Seattle, WA 98195;
[6] Apache Point Observatory, P.O. Box 59, Sunspot, NM 88349;

[7] In this paper, we use the term "Virgo overdensity" to denote both the excess stellar number density, as well as the kinematic peaks observed in the general directon of Virgo at distances $\sim 5-25$ kpc as it is unclear at present whether the two are truly distinct.

more complex large-scale structure of the Galactic stellar halo. However, given the limited extent of wide-field data available at the time, this hypothesis could not be tested conclusively.

Recently, the Eighth Data Release (DR8) of the Sloan Digital Sky Survey has become public (Aihara et al. 2011). Compared to previous releases, DR8 adds a significant new area (~ 2000 deg^2) in the southern Galactic hemisphere, as well as filling in a few "holes" in the northern footprint. Importantly, the added area allows us to conduct *symmetry studies*, model-free comparisons of stellar number densities along directions where we expect them to be the same if the halo conforms to a given shape (spherical, ellipsoidal, etc.).

In this paper, we use this newly available dataset to remeasure the size of VOD, better understand its large-scale structure, and attempt to discern between the two proposed options for its origin. We begin this analysis in Section 2 with an overview of the used stellar sample, details on the photometric parallax, and construction of stellar number density maps. Section 3 brings analysis of density maps, with special attention given to the extent of the overdensity and how it compares to surrounding area without overdensities. In the final Section we discuss the implications of presented results on the nature of Virgo.

2. DATA AND METHODOLOGY

In this section we describe characteristics of the SDSS imaging survey and the subset of its stellar sample used in this work. We discuss how the distance to each star was calculated using the photometric parallax method, paying special attention to metallicity effects. In conclusion, we show how the stellar density maps were created.

2.1. *SDSS DR8 Imaging Survey*

The Sloan Digital Sky Survey III provides an unabridged view of the night sky. Its total imaging footprint covers 14,555 deg^2, a third of the celestial sphere, including $\sim$5,200 deg^2 of imaging on the Southern Galactic Hemisphere available in Data Release 8 (Aihara et al. 2011). All of the planned imaging is now complete, but spectra will continue to be taken until the project ends in 2014. These will further enlarge the existing library which already contains spectra of 520,000 stars, 860,000 galaxies and 120,000 quasars. For a detailed overview of ongoing spectroscopic projects see Eisenstein et al. (2011).

The SDSS photometric component collects data in five optical bands: u, g, r, i and z measured in AB_ν magnitude system (Gunn et al. 1998; Fukugita et al. 1996; Gunn et al. 2006), with 95% completeness levels at magnitudes 22.1, 22.4, 22.1, 21.2, and 20.3 respectively. The latest data release has very accurate purely internal photometric calibration (Padmanabhan et al. 2008, so-called, *übercalibration*), with the same standard-star derived zeropoints used to absolutely calibrate the previous releases. Furthermore, all the imaging data was reprocessed with the new photometric pipelines, featuring enhanced sky-subtraction algorithm. Unfortunately, due to a mistake in data processing, the absolute astrometry of DR8 is less accurate than the previous releases (M. Blanton; private communication), but this is of no consequence to the work presented in this paper.

TABLE 1
Overview of Virgo Overdensity / Stellar Stream properties

Quantity	Value	Reference
Angular size (deg^2)	> 106[a]	Duffau et al. (2006)
	> 1000	Jurić et al. (2008)
	~ 760[a]	Prior et al. (2009)
	> 2000	this work
Surface brightness (mag arcsec^{-2})	32.5	Jurić et al. (2008)
Distance (kpc)	20	Newberg et al. (2002)
	19	Vivas & Zinn (2003)
	6 to 20	Jurić et al. (2008)
	19[a]	Prior et al. (2009)
	15 to 30	Brink et al. (2010)
Metallicity [Fe/H]	-1.86 ± 0.40[b]	Duffau et al. (2006)
	-1.5[c]	Jurić et al. (2008)
	-2.0 ± 0.1 (internal) ± 0.5 (systematic)[c]	An et al. (2009)
Radial velocity (km s^{-1})	99.8 ± 17.3[a]	Duffau et al. (2006)
	130 ± 10	Newberg et al. (2007)
	127 ± 10[a]	Prior et al. (2009)
	134.4 ± 14.0[a]	Casetti-Dinescu et al. (2009)
Proper motion (mas yr^{-1})	$\mu_\alpha \cos\delta = -3.50 \pm 0.85$, $\mu_\delta = 2.33 \pm 0.85$	Casetti-Dinescu et al. (2009)
Origin	Sagittarius dSph	Martínez-Delgado et al. (2007)
	dwarf galaxy	Jurić et al. (2008); Casetti-Dinescu et al. (2009); this work

[a] Quantity related to the VSS.
[b] Spectroscopically derived quantity.
[c] Photometrically derived quantity.

Importantly, the morphological star-galaxy separation algorithm is well understood and has not changed since DR2. It classifies objects as 'GALAXY' if:

$$\mathrm{psfMag} - \mathrm{cmodelMag} > 0.145. \qquad (1)$$

This admittedly simple criterion has been shown to work well for selecting clean samples of stars to $r \sim 21.5$ (Jurić et al. 2008).

2.2. *The Photometric Parallax Relation and Iterative Determination of Distances*

More than 95% of stars detected by the SDSS are on the main sequence and of similar age, therefore residing on a fairly constrained, one-dimensional, stellar locus. Provided we have a calibrated color-luminosity (or, *photometric parallax*) relation, this fact allows us to estimate both their absolute magnitudes and distances from multi-band photometry.

Once the absolute magnitude of a star is known, its distance is easily calculated using:

$$D(\mathrm{pc}) = 10^{(r-M_r)/5+1} \qquad (2)$$

which then leads to its position in Galactocentric Cartesian coordinates:

$$
\begin{aligned}
X &= R_\odot - D\cos l \cos b \\
Y &= -D\sin l \cos b \\
Z &= D\sin(b)
\end{aligned}
\tag{3}
$$

where $R_\odot$ is distance from Sun to the Galactic center and l and b are Galactic longitude and latitude, respectively.

There have been numerous efforts through studies of stellar systems with known distances (eg. nearby stars, globular clusters) yielding a number of proposed photometric parallax relations (eg. Hawley et al. 2002; Williams et al. 2002; West et al. 2005; Bilir et al. 2006). In this paper, we use the relation derived by Ivezić et al. (2008):

$$M_r(g-i, [\mathrm{Fe/H}]) = M_r^0(g-i) + \Delta M_r([\mathrm{Fe/H}]) \tag{4}$$

where the terms $M_r^0(g-i)$ and $\Delta M_r([\mathrm{Fe/H}])$ have been determined to be:

$$
\begin{aligned}
M^{\,0}_{\,r}(g-i) &= -0.56 + 14.32(g-i) - 12.97(g-i)^2 \\
&\quad +6.127(g-i)^3 - 1.267(g-i)^4 + 0.0967(g-i)^5 \quad (5) \\
\Delta\, M_r([\mathrm{Fe/H}]) &= -1.11([\mathrm{Fe/H}]) - 0.18([\mathrm{Fe/H}])^2
\end{aligned}
$$

This relation was calibrated from SDSS observations of 11 star clusters in metallicity range from +0.12 to −2.50. It builds on the previous work of Jurić et al. (2008), and is in good agreement with other proposed relations in the literature. It is expected to be accurate to $\sim 10-15\%$ (Ivezić et al. 2008), and the fact that it was directly calibrated on SDSS photometry makes it especially apropriate for use here.

While more accurate, the Ivezić et al. (2008) relation is at a disadvantage compared to, for example, the Jurić et al. (2008) due its need for the u-band photometry to determine metallicity. Given the shallower depth of the SDSS u band observations, this would effectively limit our explorations to ~ 8 kpc, heliocentric. We therefore chose not to determine metallicity from the photometry, but instead use the metallicity prior given by Ivezić et al. (2008) models to compute the $\Delta M_r([\mathrm{Fe/H}])$ needed in Equation 5. Since Ivezić et al. (2008) give the metallicity as a function of position in the Galaxy (that, in turn, depends on the absolute magnitude), this makes our problem an implicit one.

We iteratively solve for D and M_r starting with an initial guess for metallicity of $[\mathrm{Fe/H}] = -0.5$. We then compute D and M_r from the observed g, i. Next, the expected metallicity at that position in the Galaxy is drawn from distributions given by Ivezić et al. (2008, Equations 18–20), and the process is repeated until convergence is obtained. Note that since Ivezić et al. (2008) give their metallicity distributions separately for the disk and the halo, we randomly assign a star to the disk or halo component, with the weight given by their local contributions. In practice, this detail is of small importance for stars at approximate distance of the VOD, as nearly all belong to the halo.

We have compared the stellar number density dependence on the position in the Galaxy as obtained with the iterative approach, to results of Ivezić et al. (2008) as well as the result obtained using Jurić et al. (2008) photometric parallax relation. We found them to be in agreement to within ∼10% in the thin and thick disk regions, and discrepant with respect to the normalization of the halo component. In particular, while the overall halo density profile given by Jurić et al. (2008) is correct, we have found their local halo-to-disk normalization to be over-estimated by approximately a factor of three.

For Galactic models used in subsequent sections, we have lowered the halo-to-thin disk normalization parameter f_H from the Jurić et al. (2008) value to $f_H = 1.6 \times 10^{-3}$. The difference is not surprising in light of a relatively large error bar (50%) that Jurić et al. (2008) have attached to their measurement of f_H. We also note that the value used here is more consistent with those traditionally used. A formal fit for the f_H is beyond the scope of this work and will be discussed in a subsequent paper (Jurić et al.; in prep). In here, we will refer to it as the *galfast* model.

2.3. *Sample Selection and Maps of Stellar Number Density*

To be included in our sample of main sequence stars, we require the objects to be morphologically classified as 'STAR' by the SDSS pipeline, be within ∼0.32 mag of the stellar locus as defined by Equation 4 of Jurić et al. (2008), and have colors $g - r > 0$. The last cut removes extremely blue point sources, such as BHB stars or blue stragglers. We further require the objects to have $r, i < 21.5$, to restrict ourselves to the range where SDSS' morphological star-galaxy separation works well (Jurić et al. 2008). The apparent magnitudes of the resulting sample, containing ∼ 86 million objects, are then corrected for interstellar extinction using the SFD maps (Schlegel et al. 1998). Finally, we apply the iterative distance/absolute-magnitude determination procedure to all objects (stars) of this sample.

We proceed to divide up the sample in 6 absolute magnitude bins (spanning $3.5 < M_r < 9.5$), and 9 shells of heliocentric distance (spanning $2 < D/\mathrm{kpc} < 20$). The bin sizes in absolute magnitude and distance are 1 mag and 2 kpc, respectively. Results shown here contain only stars from the brightest absolute magnitude bin ($3.5 < M_r < 4.5$), which probe deepest into the stellar halo.

These data are then binned spatially, in Lambert equal area projection, and plotted in hemisphere plots. The projection poles were set to the north and south Galactic pole for examination of northern and southern SDSS data, respectively. The Lambert projection was chosen as it allows for straightforward comparison of sizes of observed structures on different parts of the sky. The map pixel scale of $dx = 1.5^\circ$ was chosen to keep most of the pixels well populated, thus reducing Poisson noise. At a central-distance bin of 9 kpc ∼70 % of pixels contain at least ∼30 stars, while at the largest distance of 19 kpc this fraction is ∼50 %.

Not all pixels on the map have been fully covered by SDSS observations. This is particularly true for pixels close to the edge of the footprint, and needs to be accounted for. For consistent comparison of data and model predictions, we compute the pixel fraction covered by the SDSS by subdividing each pixel with a 100x100 grid, and counting the number of so defined subpixels that contain at least one star. The fraction of pixel area covered by the SDSS is then approximated by the ratio of counted subpixels, to the total number of subpixels. Model predictions (discussed below) have been multiplied by this fraction.

Examples of stellar density maps thus obtained are given in Figures 1 (north Galactic hemisphere) and 2 (south Galactic hemisphere). The panels in the left column show SDSS DR8 stellar counts, while *galfast* model predictions for the same population of stars are given in the center. Model predictions give the expected number of stars in the volume determined by pixel and distance bin size. Finally, a quantitative comparison of the data and model, given by their difference normalized to the model, is shown on residual plots in the right column.

3. RESULTS

In this section we discuss the density maps constructed as described above, with emphasis on the structure of Virgo Overdensity. Previous studies found the VOD to peak at ~10 kpc. Here we present and discuss density distribution maps at two distances: 5 ± 1 kpc where we do not see signature of the VOD, and 11 ± 1 kpc where it is very prominent.

3.1. *Analysis of star counts maps*

As seen in Figure 1, the 5 kpc density map is well matched by the model prediction, resulting in mostly uniform residual map centered around zero. The density map itself reveals the bulk structure of Milky Way and our position inside it. The greatest density is observed at low Galactic latitudes ($b \lesssim 30°$) where our distance shell dips into the Galactic disk. In order to reduce the clutter and obtain a better view of the halo stars, the plots show only the region $b > 30°$. In comparison to the model predictions, we note two features on the map of residuals. First, the slight underdensity in the region heavily populated by disk stars ($0° < l < 30°$, $b < 45°$) due to model parameters tuned to best reproduce the halo, and second the Monoceros stream viewed as an overdensity on the opposite side of the map ($90° < l < 230°$, $b \lesssim 40°$).

The situation is radically different at 11 kpc. Even though the general features seen in the 5 kpc plots are also present at 11 kpc, the residuals are dominated by a large overdensity at $l \sim 300°$, $b \sim 75°$ – the Virgo Overdensity. Probability of a random fluctuation expanding over such an area is statistically insignificant.

We also present the stellar density maps of the southern Galactic hemisphere derived from SDSS DR8 data, in the same distance shells as for the northern hemisphere (Figure 2). The SDSS footprint of southern sky, limited by geographical location of the telescope, is smaller than in the north, but still large enough to resolve structures on scales as large as several hundreds deg^2. Apart from the known Hercules-Aquilae cloud ($l \sim 60°$, $b \sim -35°$) and trailing arm of the Sagittarius dwarf galaxy ($90° < l < 230°$, $b > -40°$), there appear to be no strong overdensities in the halo region. However, we do observe a curious density enhancement in the south at low latitudes in the anticenter direction. This overdensity, that could be associated with the Monoceros stream, or be a feature of the thick disk, will be analyzed in a subsequent publication. Other than the mentioned overdensities, the residual maps exhibit a very good fit to the model.

3.2. *Extent of the Virgo Overdensity*

The fact that the VOD is not only visible on the residual plot, but also as an enhancement on the density plot itself, motivates us for another, model free look at the data. This approach also reduces the dependence of our results and conclusions on the details of the analytic Galactic model.

Most overdense pixels on the VOD residual plot (lower right panel on Figure 1) are above the $l = 0°$ line. If the halo were symmetric, the halves of the plot divided by this line should also be symmetric. In Figure 3 we compare the stellar density in these halves by plotting the value of:

$$f_{W-E}(l, b) = \frac{data(l, b)}{data(360° - l, b)} - 1 \qquad (6)$$

For a given pixel at Galactic coordinates (l, b), the value of f_{W-E} is simply the normalized difference between the star counts in the pixel itself ($data(l, b)$) and its counterpart ($data(360° - l, b)$). The quantity f_{W-E} is defined only for the pixels with axisymmetrical counterparts, which results in the "bug like" shape of the plots.

The stellar number density was found to be symmetric on the order of $\lesssim 10\%$ at distances closer than 5 kpc. However, at 11 kpc the median of f_{W-E} distribution on the upper half is at $\sim 20\%$. If we adopt the definition of overdensity as density contrast (here defined with respect to the axisymmetric region) of $\geq$15%, then the total area of Virgo overdensity as measured in SDSS DR8 is ≈ 2000 deg^2, double the size previously measured (Jurić et al. 2008).

Furthermore, we see that the overdensity extends along the $l = 300°$ and 270° SEGUE stripes. This indicates that 2000 deg^2 is still only a lower limit of its actual size. We attempt to roughly estimate the area of the VOD outside the SDSS footprint by placing an ellipse encompassing most of the pixels with 40% overdensity in the SEGUE stripes as well as the overdensity in the main area of the survey. We find this area to be ~3000 deg^2, implying that approximately one third of the VOD may extend over the area where no data is currently available.

3.3. *Luminosity of the Virgo Overdensity*

To further characterize the progenitor, we estimate a lower limit on the number of stars associated with VOD. The Virgo area was conservatively limited to region subtended by: ($200° < l < 210°$, $b > 40°$), ($210° < l < 270°$, $b > 50°$) and ($270° < l < 340°$, $b > 60°$). To estimate the excess in stellar number counts, we simply subtract the pixel values in symmetric, Virgo-free area from the VOD pixels, and sum over all the pixels and distance range (7 - 19 kpc). This gives the number of VOD stars with absolute magnitude $M_r = 4.0 \pm 0.5$. Following Jurić et al. (2008), and assuming the luminosity function of VOD stars is similar to that of the halo (Jurić et al., in prep), we obtain an order-of-magnitude estimate of $\sim 10^6$ for the total number of stars present in VOD. This is consistent with numbers found for large globular clusters and dwarf galaxies.

3.4. *Test of the "Tilted Halo" model*

Given the large extent of the VOD, an attractive hypothesis is that it may not be an overdensity in the stellar

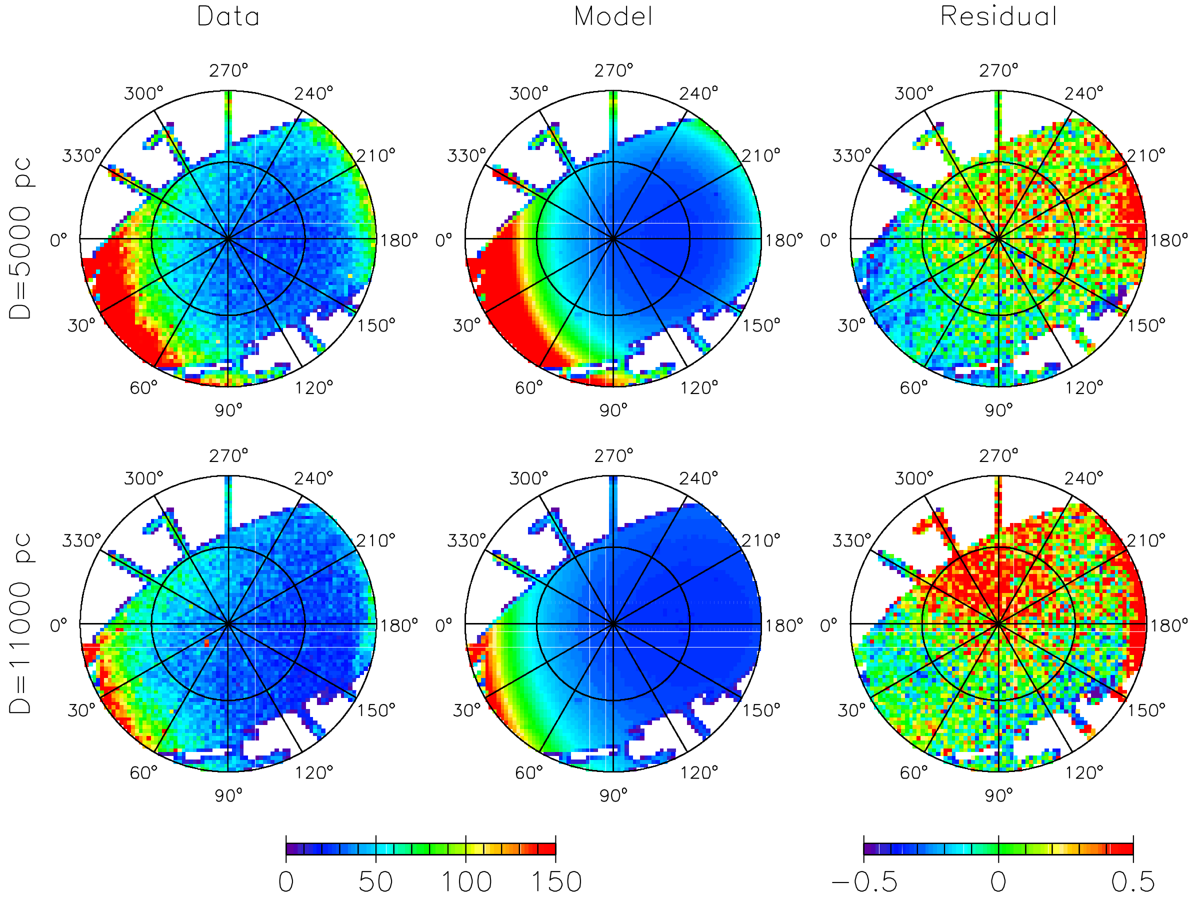

FIG. 1.— Density distribution of F stars in 2 kpc wide shells centered on 5 and 11 kpc, mapped in Lambert equal area projection with circles representing constant Galactic latitude and lines constant Galactic longitude. Disk area is excluded by plotting only latitudes higher than 30°. Left panels show SDSS DR8 imaging data, with blank areas corresponding to pixels with no data, best-fitting models updated from Jurić et al. (2008) for the same area, corrected for SDSS sky coverage, are on the middle panels, while the data - model residuals (normalized to the model) are on the right panels. At the 5 kpc distance shell, data and model are in very good agreement (apart from the disk region, which was not modeled as carefully), but the 11 kpc shell clearly shows Virgo overdensity extending over 2000 deg^2 in general direction of $l \sim 300°$, $b \sim 75°$. The Monoceros stream is visible at both distance shells as overdensity on low Galactic latitudes for $150° < l < 230°$.

halo but a signature of a more complex stellar halo density distribution. For example, proposals have been put forward that the Hercules–Aquilae cloud is a signature of dynamical interaction of the disk with the stellar bar, and not a merger event (Humphreys et al. 2011).

An oblate halo model, with axes aligned with those of the Galactic disk, does not produce an overdensity signature in maps constructed in Section 2.3. However, if its axes were not aligned with the Galactic disk (eg. if it is “tilted”), such an overdensity signature will occur (Figure 4). With the SDSS data in the southern hemisphere available for a significant portion of the sky, it is possible to test this tilted halo model by directly comparing the stellar number density above and below the Galactic plane.

We proceed similarly to steps taken in previous section and plot the values of f_{N-S} defined by:

$$f_{N-S}(l,b) = \frac{data(l,b)}{data(l,-b)} - 1 \qquad (7)$$

in Figure 5. $data(l,b)$ once again denotes stellar number count in pixel centered at (l,b) and distance of 11 kpc, analagous to the bottom rows of Figures 1 and 2. Note how the value of f_{N-S} is only defined for those pixels which have data available both above ($b > 0$) and below ($b < 0$) the Galactic plane. Although the distribution of f_{N-S} values is noisy, there is no clear over- or underdensity as would be predicted by Figure 4. This is further confirmed by the distribution of densities in pixels not affected by overdensities (excluded regions include Sagittarius dwarf galaxy at $|b| < 60°$ and $120° < l < 150°$, $45° < |b| < 60°$ and Hercules-Aquilae at circle of radius 7° around $l = 55°, b = -30°$). The distribution is slightly asymmetric, but the median is at -0.01, while the width of the distribution (with semi-interquartile range of 0.22) is consistent with the noise visible on the map of f_{N-S} values. Given the distribution centered around zero excess of north versus south, we can conclude that on the scales of ∼20 kpc, halo is symmetric with respect to the Galactic plane.

This remains true when the exercise is repeated for distance shells in $7 - 19$ kpc range. Figure 6 shows how the median of f_{N-S} distributions similar to that on Figure 5

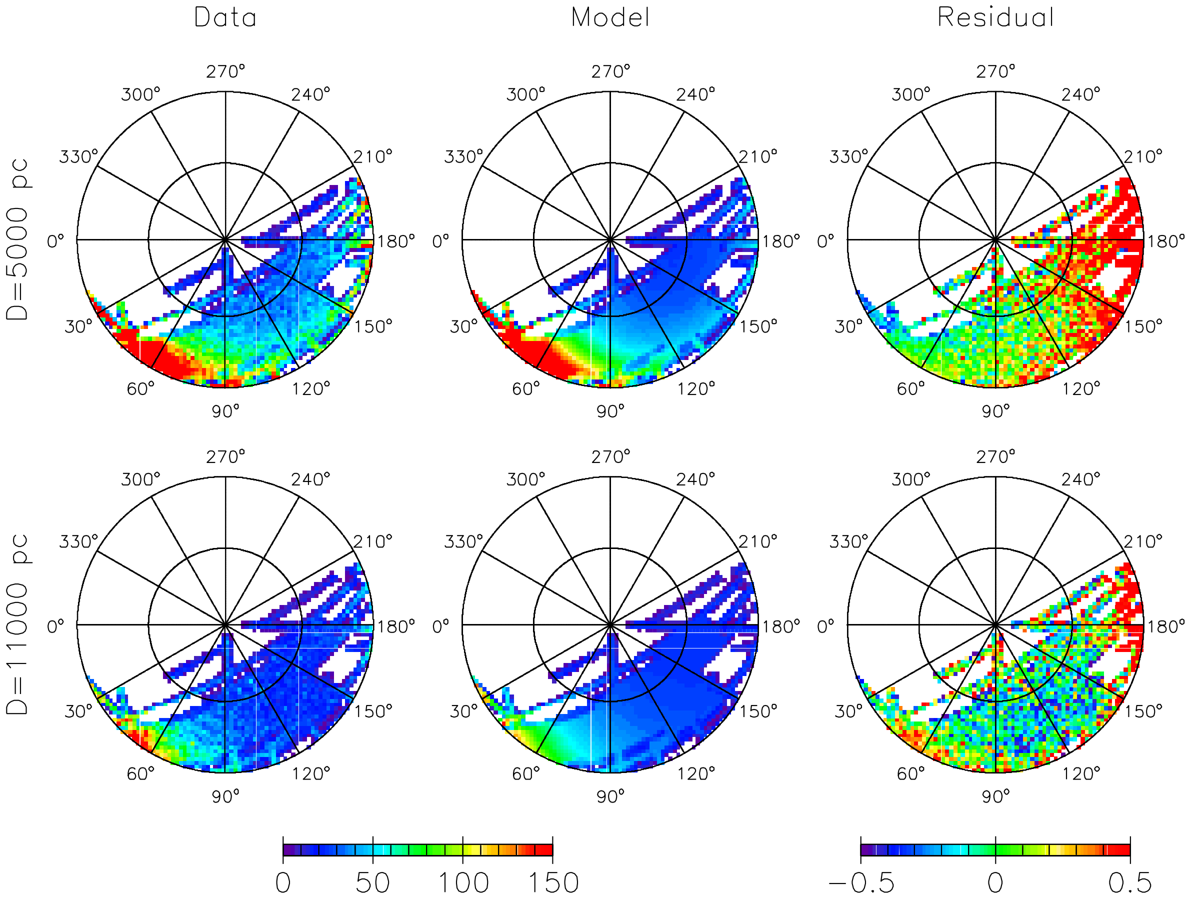

FIG. 2.— Same as Figure 1 on southern Galactic hemisphere. Apart from the enhancement at low latitudes in the anticenter region that may be related to the Monoceros stream, the Sagittarius stream ($90° < l < 230°$, $b > -40°$), and the Hercules-Aquilae cloud ($l \sim 60°$, $b \sim -35°$), no new strong excesses were detected.

changes with distance. The error bars denote the distributions' IQR. The plot shows remarkable consistency in difference of star counts between northern and southern Galactic hemisphere, the largest deviation being $\sim 10\%$ at 7 ± 1 kpc, and considerably smaller in most other distance bins.

We therefore conclude that a tilted halo cannot account for the existence and observed extent of the Virgo Overdensity.

4. DISCUSSION

Previous studies determined the distance range, radial velocities and metallicity of stars making up the VOD (see Table 1). Several authors have also reported evidence of substructure (e.g. Duffau et al. 2006). In this paper we have used the SDSS DR8 data to reasses the extent of the VOD and find it likely to extend over ~ 3000 deg^2 of the sky, three times more than the original Jurić et al. (2008) estimate.

Stellar overdensities are usually attributed to merger remnants, but VOD's size and morphology make it unlike a typical tidal stream thus calling for a more cautious interpretation. An alternative to the merger remnant hypothesis is that the VOD is a signature of a more complex global halo density distribution (for a discussion why other proposed hypotheses are less likely, see section 5.5 in Jurić et al. 2008). In this paper, we have tested whether a "tilted" halo can explain the observed signature.

Figure 4 shows schematically how a tilted halo would appear as an overdensity in Figures 3 and 5. Axisymmetric halo on the left panel would be observed as being completely symmetric in both f_{W-E} and f_{N-S} values defined earlier, but if the halo were tilted as seen in the right panel on Figure 4, a VOD-like enhancement in stellar number counts would be observed in the "western" side of the f_{W-E} plot. Halo tilt would also be evident on the f_{N-S} plot because the number counts on the "south" would be larger compared to the symmetric area on the "north". However, as we can see from Figure 6, this is not the case. In fact, given the difference in stellar number counts between north and south areas mapped by the SDSS, we can constrain any north–south halo asymmetry to be less than 10%. As the density contrast of the VOD gets as high as ∼50% (see Figure 5), it is clear this simple tilted halo model can only amount to a minor contribution to the overall enhancement in density. This leaves the merger hypothesis as the most likely[8].

While the VOD's morphology is clearly different from those of other streams (eg. Sagittarius, GD1, etc),

---

[8] While one can always invoke even more complex halo shapes to explain the observations, at some point these become unreasonably contrived.

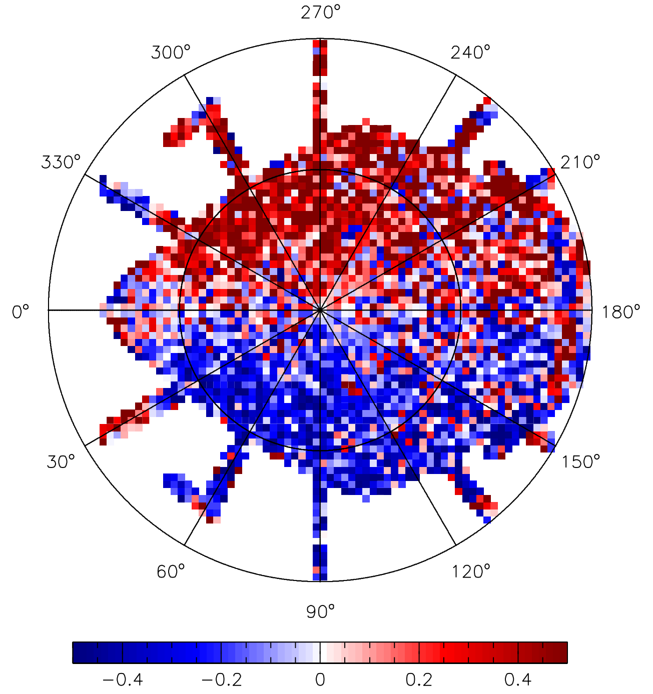

FIG. 3.— A model free confirmation of the Virgo Overdensity is given by a star count difference between $0° < l < 180°$ and $180° < l < 360°$ regions on the bottom left panel from Figure 1. The above region is $\sim 50\%$ more densely populated than the lower region. The lower limit on the overdensity area is $\sim$2000 deg^2, but note that the overdensity extends down to $b \sim 30°$ along the $l = 270°$ SEGUE stripe, so the real extent of the Virgo Overdensity might be considerably larger.

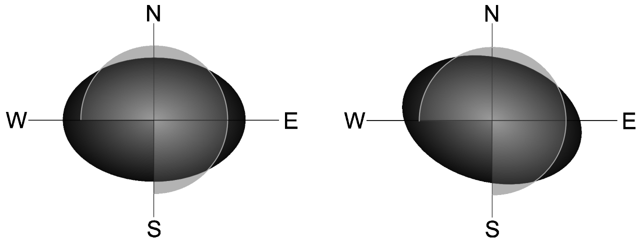

FIG. 4.— Schematic view of the cross section of oblate halo (dark gray) and spherical shell centered on the Sun (light gray). The axis connecting the Sun and the Galactic center is perpendicular to the surface of the plot. In the case of axially symmetric halo (left panel), the stellar density counts at certain distance (as marked by the light gray shell) are symmetric with respect to both $l = 0°$ line (W vs. E) and the Galactic plane (N-S). However, if the halo is tilted (right panel), so that we observe excess on the "Western" part of the sky (ie the Virgo Overdensity), then the North - South symmetry holds no longer either.

its cloudlike appearance is not entirely unique. Other such overdensities have been observed, eg. Hercules-Aquila cloud (Belokurov et al. 2007), or Triangulum-Andromeda (Rocha-Pinto et al. 2004). Similar structures appear in Galactic halo formation simulations as well. For example, the Johnston et al. (2008) simulations modeled to match observed properties of Local Group galaxies predict several cloud-like morphologies with surface brightness $\approx$32.5 mag arcsec^{-2} in a Milky Way type galaxy. This is broadly consistent with what we see in Virgo Overdensity; however, we do find traces of VOD as close as 7 kpc from the Galactic center, closer than the simulations would predict. Given the simplicity of the simulations, this may not be a serious issue.

Furthermore, the accretion origin of the VOD is consistent with kinematic measurements of an RR Lyrae star assumed to belong to the Virgo Stellar Stream (Casetti-Dinescu et al. 2009). Based on the radial velocity and proper motion measurement with a baseline of a century, Casetti-Dinescu et al. (2009) have determined the orbit of an VSS RR Lyrae, having $r_{peri} = 11 \pm 1$ kpc, $r_{apo} = 89^{+52}_{-32}$ kpc, and a period of $T = 1.2^{+0.6}_{-0.4}$ Gyr. The measured orbit passes through the VOD, indicating that VOD and VSS may be connected structures with a common origin. Also, the high eccentricity of the orbit is consistent with the observed high eccentricities in simulated merger events that result in cloudlike structures.

Taken together, all these lines of evidence point to the VOD being a signature of a high eccentricity merger event observed at perigalacticon. Future kinematic studies are the best way to further verify this conclusion.

The authors wish to thank Marla Geha, Dana Casetti, and Nhung Ho for reading the early versions of the manuscript and providing thoughtful comments, and Branimir Sesar for help with accessing the SDSS data. M.J. gratefully acknowledges support by NASA through Hubble Fellowship grant #HST-HF-51255.01-A awarded by the Space Telescope Science Institute, which is operated by the Association of Universities for Research in Astronomy, Inc., for NASA, under contract NAS 5-26555.

Funding for SDSS-III has been provided by the Alfred P. Sloan Foundation, the Participating Institutions, the National Science Foundation, and the US-Department of Energy. The SDSS-III Web site is http://www.sdss3.org/.

SDSS-III is managed by the Astrophysical Research Consortium for the Participating Institutions of the SDSS-III Collaboration including the University of Arizona, the Brazilian Participation Group, Brookhaven National Laboratory, University of Cambridge, University of Florida, the French Participation Group, the German Participation Group, the Instituto de Astrofisica de Canarias, the Michigan State/Notre Dame/JINA Participation Group, Johns Hopkins University, Lawrence Berkeley National Laboratory, Max Planck Institute for Astrophysics, New Mexico State University, New York University, Ohio State University, Pennsylvania State University, University of Portsmouth, Princeton University, the Spanish Participation Group, University of Tokyo, University of Utah, Vanderbilt University, University of Virginia, University of Washington, and Yale University.

REFERENCES

Aihara, H., et al. 2011, ApJS, 193, 29
An, D., et al. 2009, ApJ, 707, L64
Belokurov, V., et al. 2006, ApJ, 642, L137
—. 2007, ApJ, 657, L89
Bilir, S., Karaali, S., Ak, S., Yaz, E., & Hamzaoğlu, E. 2006, NewA, 12, 234
Brink, T. G., Mateo, M., & Martínez-Delgado, D. 2010, AJ, 140, 1337

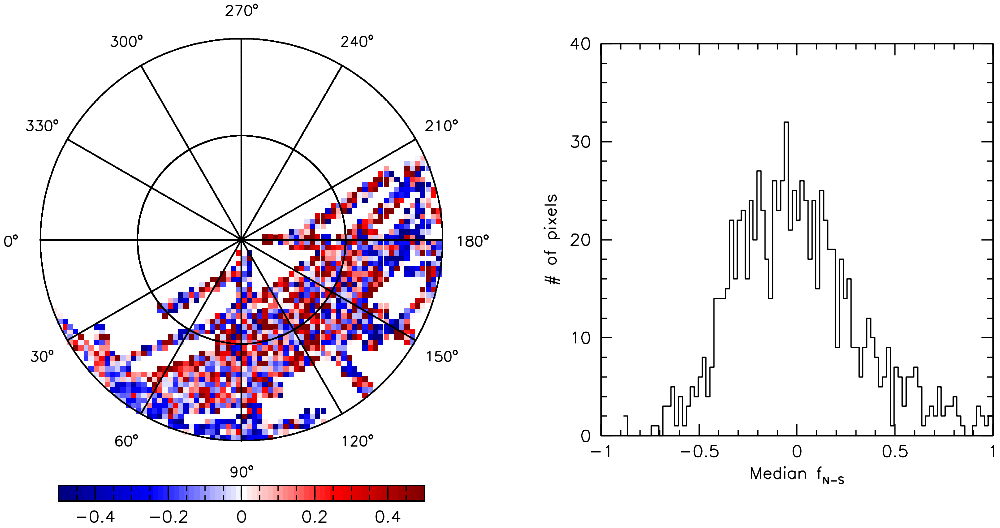

FIG. 5.— A map of difference in star counts in northern and southern Galactic hemisphere (see bottom left panels on Figures 1 and 2, respectively), normalized to the south. A very good match of the number counts over 20 kpc range provides strong constraints on the halo symmetry with respect to the Galactic plane and disfavors the tilted halo interpretation for the Virgo Overdensity.

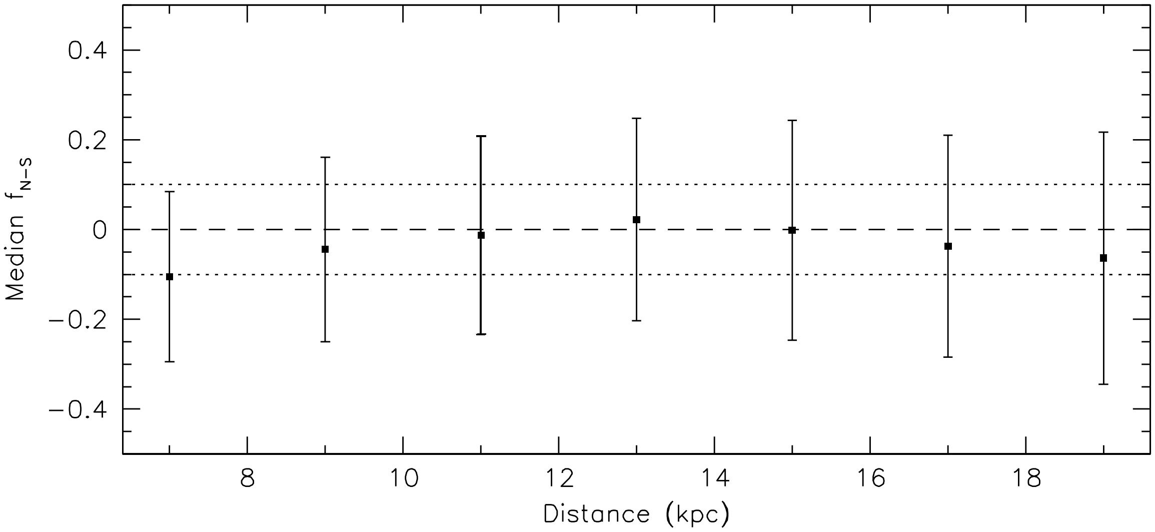

FIG. 6.— Symmetry of stellar halo with respect to the Galactic plane as a function of distance from the Sun. f_{N-S}, as defined in Equation 7, is here computed only for the areas not contaminated by Hercules–Aquilae cloud and Sagittarius stream. The error bars represent the semi-interquartile ranges of the f_{N-S} distribution. The biggest deviation from symmetry (denoted by the dashed line at zero) is ∼ 10% (dotted line), found in the 7 kpc distance bin. Note there are no strong asymmetry signatures in the distance range where the VOD is prominent.

Casetti-Dinescu, D. I., Girard, T. M., Majewski, S. R., Vivas, A. K., Wilhelm, R., Carlin, J. L., Beers, T. C., & van Altena, W. F. 2009, ApJ, 701, L29

Duffau, S., Zinn, R., Vivas, A. K., Carraro, G., Méndez, R. A., Winnick, R., & Gallart, C. 2006, ApJ, 636, L97

Eisenstein, D. J., et al. 2011, AJ, 142, 72

Fardal, M. A., Guhathakurta, P., Babul, A., & McConnachie, A. W. 2007, MNRAS, 380, 15

Ferguson, A. M. N., Irwin, M. J., Ibata, R. A., Lewis, G. F., & Tanvir, N. R. 2002, AJ, 124, 1452

Fukugita, M., Ichikawa, T., Gunn, J. E., Doi, M., Shimasaku, K., & Schneider, D. P. 1996, AJ, 111, 1748

Gunn, J. E., et al. 1998, AJ, 116, 3040

—. 2006, AJ, 131, 2332

Hawley, S. L., et al. 2002, AJ, 123, 3409

Humphreys, R. M., Beers, T. C., Cabanela, J. E., Grammer, S., Davidson, K., Lee, Y. S., & Larsen, J. A. 2011, AJ, 141, 131

Ibata, R., Irwin, M., Lewis, G., Ferguson, A. M. N., & Tanvir, N. 2001, Nature, 412, 49

Ivezić, Ž., et al. 2000, AJ, 120, 963

—. 2008, ApJ, 684, 287

Johnston, K. V., Bullock, J. S., Sharma, S., Font, A., Robertson, B. E., & Leitner, S. N. 2008, ApJ, 689, 936

Jurić, M., et al. 2008, ApJ, 673, 864

Kalirai, J. S., Guhathakurta, P., Gilbert, K. M., Reitzel, D. B., Majewski, S. R., Rich, R. M., & Cooper, M. C. 2006, ApJ, 641, 268

Majewski, S. R., Skrutskie, M. F., Weinberg, M. D., & Ostheimer, J. C. 2003, ApJ, 599, 1082

Martínez-Delgado, D., Peñarrubia, J., Jurić, M., Alfaro, E. J., & Ivezić, Z. 2007, ApJ, 660, 1264

Morrison, H. L., Harding, P., Hurley-Keller, D., & Jacoby, G. 2003, ApJ, 596, L183

Newberg, H. J., Yanny, B., Cole, N., Beers, T. C., Re Fiorentin, P., Schneider, D. P., & Wilhelm, R. 2007, ApJ, 668, 221

Newberg, H. J., et al. 2002, ApJ, 569, 245

Padmanabhan, N., et al. 2008, ApJ, 674, 1217

Prior, S. L., Da Costa, G. S., Keller, S. C., & Murphy, S. J. 2009, ApJ, 691, 306
Rocha-Pinto, H. J., Majewski, S. R., Skrutskie, M. F., & Crane, J. D. 2003, ApJ, 594, L115
Rocha-Pinto, H. J., Majewski, S. R., Skrutskie, M. F., Crane, J. D., & Patterson, R. J. 2004, ApJ, 615, 732
Schlegel, D. J., Finkbeiner, D. P., & Davis, M. 1998, ApJ, 500, 525
Skrutskie, M. F., et al. 2006, AJ, 131, 1163
Vivas, A. K., Jaffé, Y. L., Zinn, R., Winnick, R., Duffau, S., & Mateu, C. 2008, AJ, 136, 1645
Vivas, A. K., & Zinn, R. 2003, Mem. Soc. Astron. Italiana, 74, 928
Vivas, A. K., et al. 2001, ApJ, 554, L33
West, A. A., Walkowicz, L. M., & Hawley, S. L. 2005, PASP, 117, 706
Williams, C. C., et al. 2002, in Bulletin of the American Astronomical Society, Vol. 34, American Astronomical Society Meeting Abstracts, 115.11–+
Yanny, B., et al. 2000, ApJ, 540, 825
York, D. G., et al. 2000, AJ, 120, 1579
Zucker, D. B., et al. 2004, ApJ, 612, L121